INTERNATIONAL JOURNAL OF ENERGY RESEARCH
Int. J. Energy Res., **23**, 125–139 (1999)

CHEMICAL DESCRIPTION OF SPRING WATERS FROM THE TUTUPACA AND RIO CALIENTES (PERU) GEOTHERMAL ZONES

R. M. BARRAGÁN R[1], V. M. ARELLANO G[1], P. BIRKLE[1], E. PORTUGAL M[1] AND G. DÍAZ H[2]

[1] *Instituto de Investigaciones Eléctricas, Unidad de Geotermia, Reforma 113, Col. Palmira, C.P. 62490, Temixco, Morelos, México*
[2] *CENERGIA, República de Perú*

SUMMARY

Analysis of chemical data from 34 spring samples from the Tutupaca and Río Calientes (Republic of Perú) geothermal zones is presented in this paper. The main objective of the work was to characterize geothermal resources to be exploited in the future. The investigated zones were: Tutupaca and Río Calientes-Ancocollo-Challapalca. Thermal waters from Tutupaca showed low pH values and they were classified as sulphate type waters. Thermal springs from the Río Calientes zone showed almost neutral pH values and they were classified as sodium chloride type waters with a probably geothermal origin. Reservoir temperatures were estimated and the results indicated that water–rock equilibrium in the hydrothermal system was not completely attained. Taking into account the chemical composition of some equilibrated or 'mature' waters from the Río Calientes zone, reservoir temperatures in the range of 210–240°C were estimated. Mixing models based on silica, chloride and specific enthalpy of the samples were used to estimate the composition of the reservoir liquid. Isotopic data showed oxygen-18 shift for the waters from Río Calientes-Ancocollo regarding the waters from Tutupaca zone which were found on the world meteoric line. Copyright © 1999 John Wiley & Sons, Ltd.

KEY WORDS: geothermal energy; thermal springs; reservoir temperatures; mixing models; Republic of Perú

1. INTRODUCTION

Previous geochemical studies of thermal springs from the Republic of Perú (Mercado and Nieva, 1980), showed the occurrence of zones with a good geothermal potential mainly in the southern part of the country. Scandiffio *et al.* (1992), carried out a geochemical study of the Tutupaca-Río Calientes-Calacoa and Challapalca-Paucarani zones.

The samples for this study were collected and analysed by CENERGIA (Centro de Conservación de Energía y del Ambiente) (ELECTROPERU, 1994), the electrical service company in Perú. The zones investigated were Tutupaca and Río Calientes-Ancocollo-Challapalca in the SE part of the country.

In 1996 the geochemical technical staff from the IIE visited the zones and samples for isotopic (oxygen and deuterium) analyses from 13 selected places were collected. Isotopic data provided by CENERGIA (analyses performed by the International Atomic Energy Agency) were also interpreted. The samples from Tutupaca and Callazas zones were found in the meteoric line trend while the samples from Río Calientes showed oxygen shift (more than two units) which is characteristic of underground waters at high temperatures. A reservoir temperature for Tutupaca was estimated as 191°C. As very low reservoir temperatures were estimated by using both silica and potassium geothermometers it was concluded that hot reservoir fluids ascend to a shallower reservoir where fluid-rock re-equilibration seems to occur. For the Río Calientes zone

---

* Correspondence to: Rosa Maria Barragán R., Instituto de Investigaciones Eléctricas, Unidad de Geotermia, Reforma 113, Col. Palmira, C.P. 62490, Temixco, Morelos, México. Email: rmb@iie.org.mx

Contract grant sponsor: Secretaria de Relaciones Exteriores (México)

CCC 0363-907X/99/020125-15$17.50

Received 10 June 1998
Accepted 24 July 1998

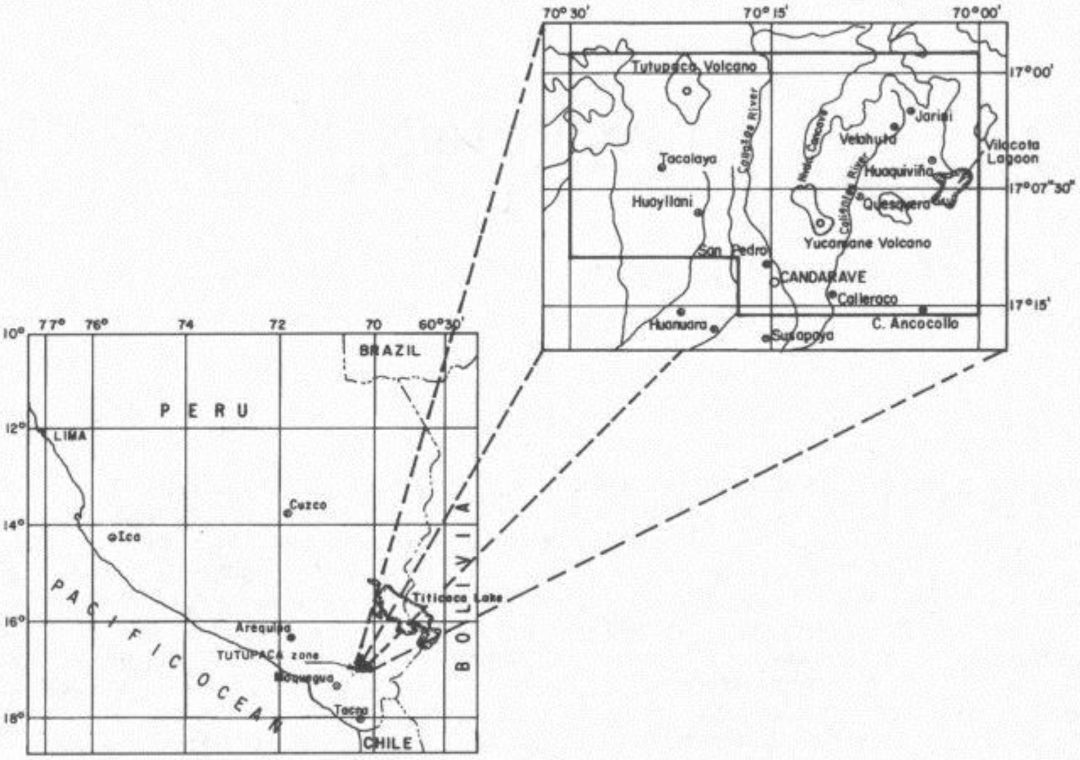

Figure 1. Location of the sampled zones

a reservoir temperature of 193°C was estimated. Temperature estimations for this zone were in agreement among different geothermometers.

Figure 1 shows the location of the sampled zones. As it was pointed out by CENERGIA, the springs distribution is controlled by andine (NW-SE) and anti-andine fault systems. The springs in the area of Río Calientes are located along SW-NE and SE-NW faults. Thermal activity is also shown by mineral deposition in zones where no surface springs occur. CENERGIA reported that this could be due either to the occurrence of a cooling process in the system or to the lack of enough recharge entering the aquifer. Data for this work were provided by CENERGIA.

2. GEOLOGICAL SETTING

The Tutupaca area is located in the southern part of Peru in the high part of the Andean Western Cordillera, near the border to Chile and Bolivia. During Mesozoic time, the study zone was mainly covered by terrigenous sediments, which were intensively deformed and folded. Intercalations of sandstones, gray shales and limestones of the Ataspace Formation were deposited during Upper Jurassic, followed by fine to medium grained sandstones of the Chachacumane Formation during Cretaceous time period. The latter one, which declines with 70–80° towards the SW, crops out with a minimum thickness of 120 m in the southeastern part of the study area. Strong volcanic activity from Early Tertiary up to recent times caused the widespread distribution of volcanic deposits in the southern part of Peru.

An angular discordance separates the Oligocene Huilacollo Formation from the anterior units. Two facies can be distinguished in E–W direction: a volcanic-sedimentary sequence in the eastern part (Chuquitira-Cano-Cucho), formed by lapillis, volcanic breccias and minor tuffs, and a volcanic sequence with

Table 1. Chemical composition (mg/kg) of samples from Tutupaca and other related zones, Perú

Sample	Code	T(°C)	pH (25°C)	Eh	COND (mS*/cm)	CO_2	HCO_3 calcul.	Cl	SO_4	F	NH_3	SIO_2	Na	K	Ca	Mg	Li
Centre Tutupaca																	
TU	12	43	2·2	62	2·78	24	33	256	1051	0·52	0·40	201	180	19	150	40	0·8
TU	13	51	2·2	411	2·90	15	21	257	1090	0·39	0·27	222	190	17	153	43	0·7
TU	23	58	2·2	341	2·96	23	32	271	1033	0·92	0·38	216	185	23	150	40	0·7
TU	29	48	3·2	n.d.	2·34	23	32	354	816	2·06	0·20	212	250	50	138	33	1·0
NE Tutupaca, Rio Callazas North																	
TU	40B	21	8·4	100	0·28	54	75	26	41	0·09	0·30	47	50	2	16	2	0·1
TU	39	17	8·1	166	0·22	62	86	16	38	0·12	0·25	5	43	3	15	3	0·1
TU	35	13	7·1	175	0·66	126	175	16	225	0·09	0·22	8	43	115	60	31	0·1
TU	34	24	6·9	138	1·20	580	804	53	345	0·16	0·39	126	110	26	83	46	0·2
TU	30	19	8·2	182	0·80	470	652	7	78	0·14	0·25	83	90	22	48	35	0·1
East Tutupaca, Rio Callazas																	
CA	6	64	7·0	332	1·82	221	306	391	156	1·00	0·20	145	295	26	44	15	1·9
CA	7	75	3·7	389	2·94	6	8	735	592	1·47	0·12	289	450	75	89	21	2·8
CA	5	77	3·5	350	3·20	15	21	760	597	1·10	0·34	293	455	75	90	21	2·8
CA	4	n.d.	3·8	470	3·74	11	15	897	710	1·00	0·12	201	575	83	105	25	2·9
TU	60	53	7·1	157	1·64	485	672	353	195	0·42	0·33	165	248	30	52	23	1·3
CA	1	35	7·4	185	1·20	218	302	194	177	0·44	0·10	133	170	19	47	20	0·8
CA	2	54	7·3	174	1·80	261	362	332	227	0·38	0·06	173	275	39	54	24	1·6
South Tutupaca, Pampa Turun Turun																	
TU	3	26	6·4	206	0·86	540	749	61	201	0·23	0·35	130	83	14	63	24	0·2
West Tutupaca, Quebrada Tecalaya																	
GN	x	27	6·8	n.d.	0·98	562	779	11	214	0·11	0·11	126	118	23	58	38	0·0
GN	4	13	7·7	n.d.	0·20	83	115	11	33	n.d.	0·95	43	24	60	13	3	0·0
GN	1	45	7·0	69	2·28	604	837	452	300	0·67	0·70	107	405	34	50	6	1·8
GN	2	47	7·2	136	2·46	651	903	490	319	0·78	0·14	107	450	34	50	6	1·9
GN	5	33	7·1	n.d.	2·92	569	789	612	357	0·78	0·00	105	510	42	52	10	1·7
GN	10A	55	7·0	145	3·04	572	793	622	409	0·87	0·60	130	600	40	66	6	2·5
Rio Callentes																	
RC	1	87	8·2	91	6·42	70	97	3340	61	1·70	0·16	293	1160	123	26	0·3	13·0
RC	12	87	7·3	172	6·44	101	140	3320	97	1·90	0·32	302	1220	95	37	0·2	14·0
RC	15	88	7·3	158	4·78	150	208	1500	107	0·95	0·24	227	780	58	48	3	9·0
RC	17	29	7·5	200	2·02	130	180	724	85	0·27	0·34	167	315	31	34	9	2·7
RC	29	54	7·7	203	1·34	111	154	387	25	0·15	0·09	145	205	34	17	6	1·7
Ancocollo																	
AN	2	86	8·0	34	6·08	93	129	2100	197	1·81	0·94	203	1160	98	31	0·1	12·0
AN	3	80	7·5	14	6·48	198	275	2380	200	1·68	1·33	163	1220	105	51	2	13·0
AN	4	88	7·3	4	6·52	166	230	2310	207	1·84	1·20	180	1220	95	50	2	13·0
East Ancocollo																	
AN	1	46	7·0	129	1·78	715	991	294	144	0·38	0·50	180	225	23	83	53	1·3
AN	17	83	3·6	398	4·26	7	10	1150	631	0·59	0·43	178	570	93	138	23	4·3
Challapalca																	
KA		86	8·2	168	7·02	43	60	2950	75	1·10	1·10	295	1320	87	69	0·5	14·3

trachiandesites and andesites in the area of Ichicollo-Cocaachi. Its major expression can be observed in the zone of Cocaachi-Ichicollo. During Miocene, the effusion of aproximately 600 m of ignimbrites (Huaylillas Formation) caused the cover of the underlying layers. The unit crops out in the southern part of the study zone (Sheet Yucamane and San Pedro). No compressive deformation occurred to this unit, except ruptures by brittle faults. Birkle *et al.* (1996) proposed the possible sealing of a potential geothermal reservoir, which consists of the Huilacollo Formation and underlying units, by ignimbrites of the Huaylillas Formation.

The Capillune Formation of the Maure Group with a high storage capacity forms the principal shallow aquifer unit of the region. The main springs discharge within the Valleys of the Calientes River and Callazas River as part of the Capillune aquifer. A samitic-ruditic facies with sandstones, conglomerates tuffs and breccias in the southern part can be distinguished from a tuff facies towards the north. The Lower Pliocene formation with a thickness of 80 –130 m is exposed throughout the entire area, mainly in natural creeks and depressions.

The Barroso Group of Upper Pliocene to Pleistocene age covers more than 70% of the surface area, thus representing the principal unit. The group can be subdivided in two series, the Antique Barroso and the Recent Barroso. The first one comprises highly destructed volcanic edifices with a high grade of glacial erosion as products of the Pleistocene glaciations. The up to 800 m thick series includes the systems of Tacalaya, Chuquiananta, Estrone, Nazaparco, López Extraña, Suri and Isccampu Pasarani, which mainly consist of andesitic lavas, pyroclastics and breccias.

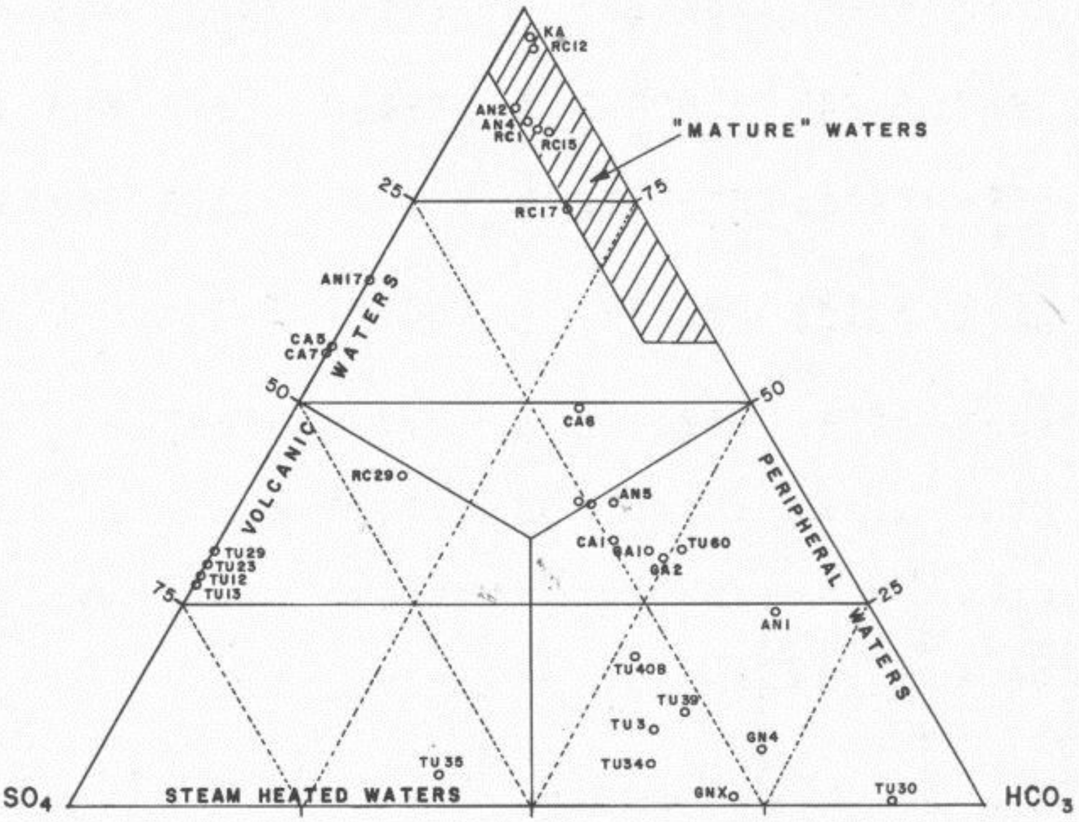

Figure 2. Relative Cl–SO_4–HCO_3 content for the samples

The Recent Barroso series of Pleistocene age unifies volcanic buildings with a relatively conserved original shape, including the systems of Tutupaca, Yucamane and Inciensocucho. The stratigraphy with a maximum thickness of 700 m consists of lava flows, traquiandesitic, dacitic and rhyodacitic domes with white, vitroclastic tuffs as base unit.

The formation of various stratovolcanos in NW–SE direction can be ascribed to the existence of andine and anti-andine fault systems, which originate mountains with elevations between 4000 and 5815 m a.s.l.

The abundance of recent volcanic features, such as domes, collapse craters, calderas, shield volcanos and thick pyroclastic sequences indicate the existence of a still active magma chamber. Also, the rise of deep circulating fluids and vapour is facilitated by the occurrence of major structural settings, especially by andine and anti-andine fault systems.

3. CHEMICAL COMPOSITION OF FLUIDS

Chemical composition of samples is given in Table 1. Many of the samples were taken at boiling temperature (88°C) and near neutral pH values were measured. Some samples from Tutupaca Centre showed low pH values.

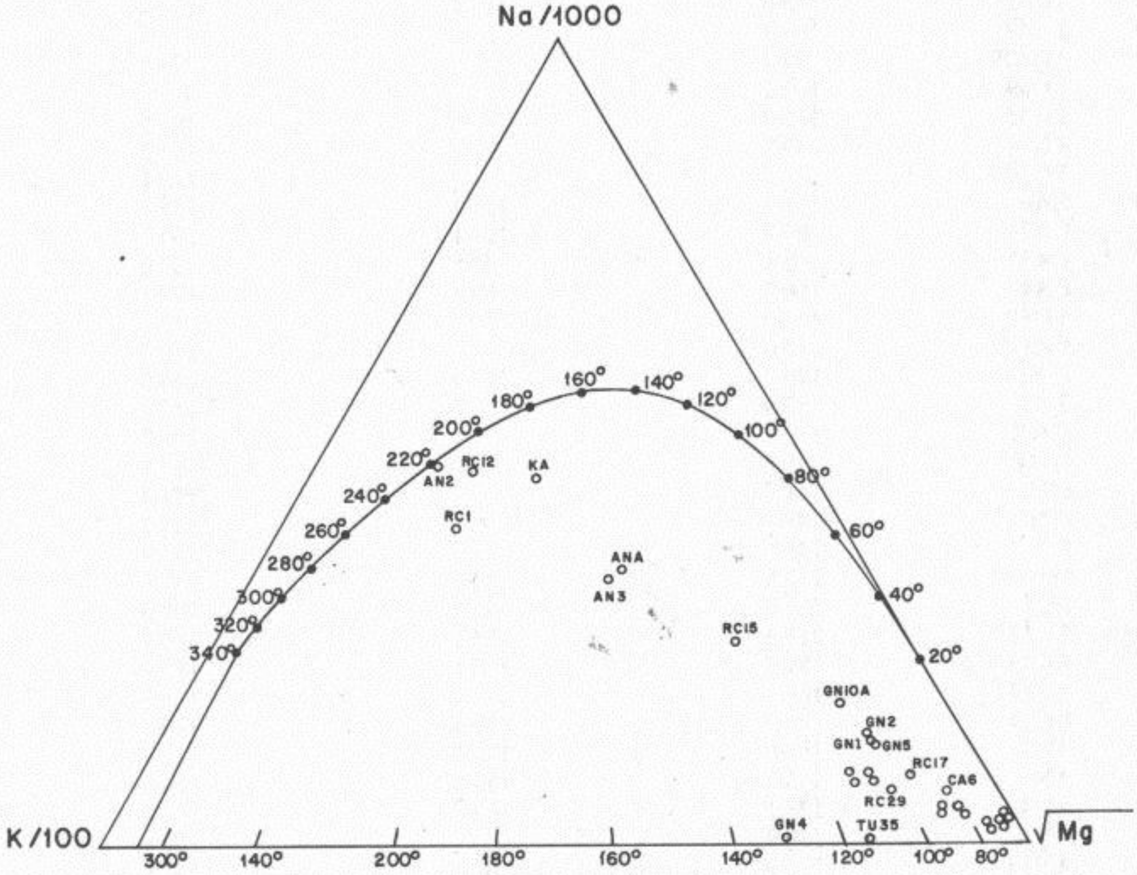

Figure 3. Relative Na–K–Mg content for the samples

Relative Cl–SO_4–HCO_3 composition for the samples is shown in Figure 2 (after Giggenbach, 1988). Only few samples (AN2, AN4, RC1, RC12, RC15, RC17 and KA), from Río Calientes zone are located in the area related to 'mature' waters. Samples from Tutupaca Centro (TU12, TU13, TU23, TU29 and TU35), are located mainly on the sulphate region where waters are classified as volcanic. Low pH values for these waters are due to absorption of magmatic gases and the sulphate content is explained by oxidation of H_2S to SO_4. All the other samples are located on the bicarbonate region and they are known as 'peripheral' waters. For these waters it is supposed that the high content of HCO_3 is due to the absorption of deep CO_2.

Figure 3 shows the relative Na–K–Mg content for the samples (after Giggenbach, 1988). Groundwaters and springs are usually found close to the Mg corner while geothermal weirbox samples are found on the full equilibrium line. As shown in the diagram, only sample AN2 is located on this line (at 219°C); but the samples identified before as 'mature' are located on the partial equilibrium area.

Table 2. Reservoir temperatures estimated by silica geothermometers

Sample	*T* (conductive cooling) (°C)	*T* (adiabatic cooling) (°C)	*T* (°C) (Giggenbach)
TU12	180·9		172·1
TU13	187·9	175·2	180·8
TU23	186·0	173·6	178·4
TU29	184·7		176·7
TU40B	99·4		74·5
TU39	109·2		85·9
TU35	125·9		105·6
TU34	150·7		135·2
TU30	127·2		107·1
CA6	159·4	151·3	145·6
CA7	207·7	191·1	205·7
CA5	208·8	192·0	207·0
CA4	180·9	169·4	172·1
TU60	167·6	158·3	155·7
CA1	154·0		139·2
CA2	170·7	160·9	159·5
TU3	152·6		137·5
GNX	150·7		135·2
GN4	95·4		69·9
GN1	141·2		123·7
GN2	141·2		123·7
GN5	140·1		122·4
GN10A	152·6	145·4	137·5
RC1	208·8	192·9	207·0
RC12	211·2	194·1	210·1
RC15	189·5	176·1	182·8
RC17	168·4		156·7
RC29	159·4	151·3	145·6
AN2	181·6	170·1	172·9
AN3	166·8	157·6	154·8
AN4	173·4	163·5	162·8
AN1	188·9		162·8
AN17	172·6	162·5	161·9
KA	209·3	192·5	207·7

4. GEOTHERMOMETRY

4.1. Silica geothermometers

Results for silica geothermometers (after Fournier and Potter II, 1982; Giggenbach, 1991), are given in Table 2. As is seen, moderate temperatures for the reservoir were calculated. Quartz geothermometer provided a maximum value of 211°C for one sample from the Río Calientes zone, assuming conductive cooling. By assuming adiabatic cooling reservoir temperatures are lower. Giggenbach's silica geothemometer considers spring fluids to be in equilibrium with either amorphous silica or chalcedony. This geothermometer is in agreement with the results from the quartz conductive cooling geothermometer for temperatures above 200°C.

4.2. Cation geothermometers

The following cation geothermometers were calculated (see Table 3) : Na/K (F) (Fournier, 1979a); Na–K– Ca (Fournier and Truesdell, 1973), Mg correction (Fournier and Potter II, 1979); the

Table 3. Reservoir temperatures (°C) estimated by cationic geothermometers

MUESTRA	Na/K (F)	Na–K–Ca	CORR. Mg	TCCG	Na/K (G)	K/Mg (G)
TU12	221·9	82·0	68·5	33·3	236·7	65·1
TU13	207·8	78·5	67·2	32·6	223·6	61·8
TU23	236·6	88·8	66·6	34·8	250·3	69·4
TU29	284·9	209·5	75·3	41·9	294·4	90·8
TU40B	NA	46·5	46·5	22·6	168·4	48·9
TU39	188·1	57·6	57·6	26·7	205·1	53·1
TU35	NA	390·7	130·1	50·7	NA	114·9
TU34	304·1	208·1	26·8	39·4	311·8	70·7
TU30	308·1	211·7	19·5	41·2	315·4	69·9
CA6	206·6	176·6	53·9	44·2	222·4	84·2
CA7	265·3	214·9	90·7	177·9	293·3	108·1
CA5	264·2	214·3	91·1	177·5	275·6	108·1
CA4	250·9	209·3	87·2	173·6	263·4	108·5
TU60	234·1	189·3	40·4	44·7	248·0	82·4
CA1	226·9	178·9	38·0	40·4	241·3	73·1
CA2	249·1	200·1	44·3	46·9	261·8	88·5
TU3	266·6	82·5	54·4	34·3	277·8	64·0
GNX	282·0	201·5	21·1	41·0	291·9	70·0
GN4	NA	389·9	262·8	49·9	NA	130·8
GN1	202·6	178·6	120·5	189·8	218·7	103·4
GN2	194·3	174·8	119·3	181·7	210·9	103·4
GN5	201·1	181·3	95·3	188·3	217·3	102·2
GN10A	184·7	170·8	131·1	172·3	201·9	108·0
RC1	222·3	219·2	213·3	209·1	237·0	201·3
RC12	196·6	197·8	197·8	184·0	213·1	198·9
RC15	193·0	184·2	162·2	180·4	209·7	129·7
RC17	215·8	186·2	77·9	155·1	231·0	95·4
RC29	264·8	215·4	86·9	50·8	276·2	103·4
AN2	203·1	203·3	203·3	190·3	219·2	216·0
AN3	204·7	200·5	192·7	191·8	227·1	156·9
AN4	196·6	194·8	186·8	184·0	213·1	153·3
AN1	219·1	174·1	18·9	40·7	234·1	66·2
AN17	263·1	213·9	110·9	179·9	274·7	113·0
KA	183·9	183·9	180·8	171·5	201·1	176·1

cationic composition geothermometer CCG (Nieva and Nieva, 1987); Na/K (G) and K/Mg (Giggenbach, 1988).

Cationic geothermometers provide a wide range of temperature values. Too low temperature values (sometimes meaningless), are obtained by using geothermometers that consider Mg such as; Mg correction, CCG and K/Mg. This was expected since only few samples were classified as 'mature'. The CCG preclassifies the samples according to the Na–K–Ca–Mg relative content. For high Mg waters a low temperature is calculated, while for low Mg, high temperature waters, the expression for the CCG depends only on the Na/K ratio. Considering Na/K geothermometers qualitative results were as follows. NA/K (G) provided the higher temperatures compared with NA/K (F) and this in turn, gave higher temperatures than those obtained using the CCG.

Figure 4 was proposed by Giggenbach (1995) in order to study spring samples where water-rock full equilibrium is not attained. This diagram relates the Na–K–Ca–Mg composition for the samples and it allows the most likely reservoir temperature to be estimated. In the diagram an almost vertical trend for the samples towards the horizontal axes is observed. Sample AN2 is located on the equilibrium line while

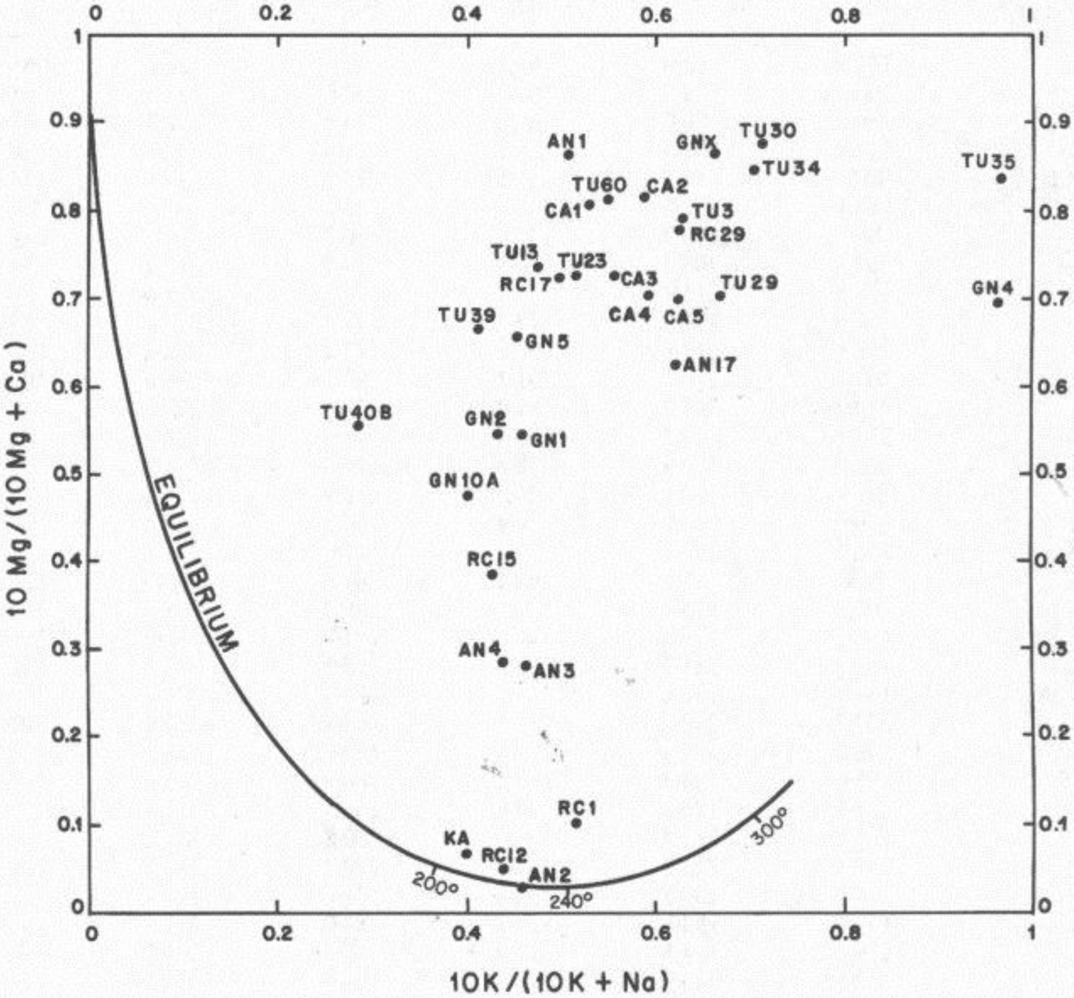

Figure 4. Na–K– Ca–Mg equilibrium temperatures for the samples

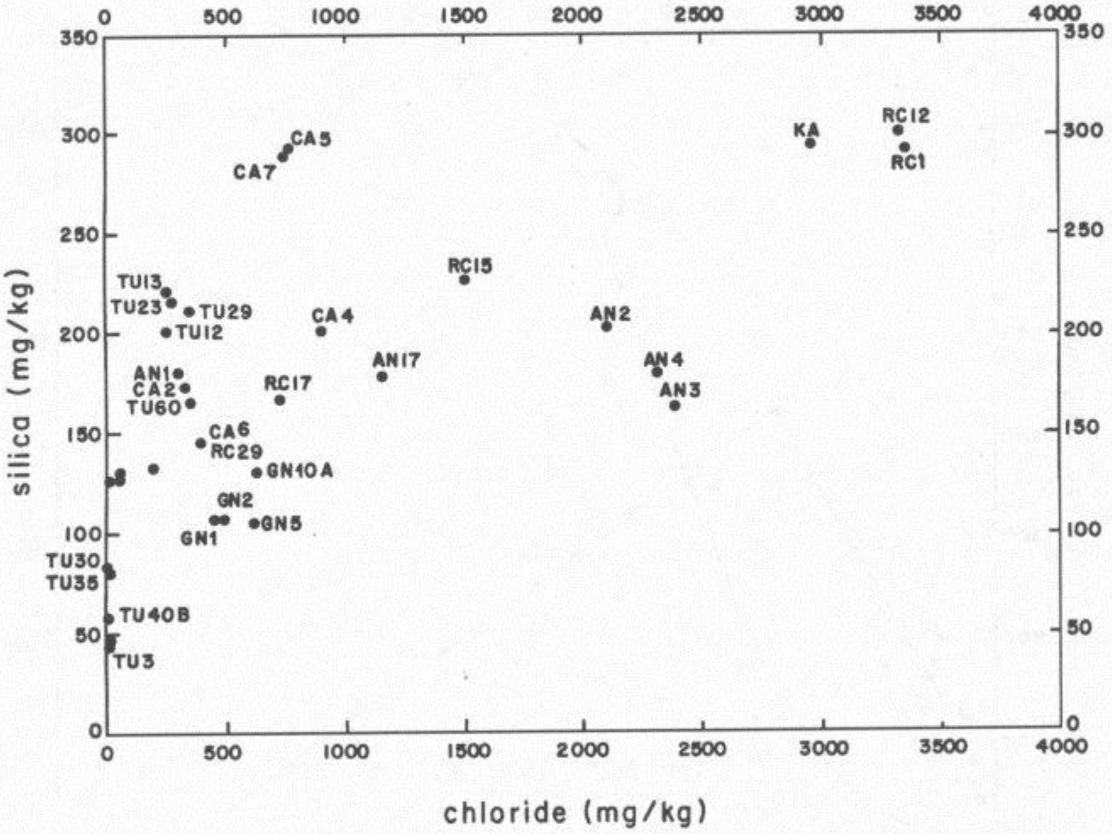

Figure 5. Silica vs. chloride concentration plot for the samples

samples RC1, RC12 and KA are located very close to it. The location of these samples show reservoir temperatures in the range of 210–240°C. Samples TU35 and GN4 are located to the right-hand side from the region above the equilibrium curve. For these samples, the Na–K–Ca geothermometer provided very high reservoir temperature, above the critical point.

5. MIXING MODELS

A relationship between silica and chloride for the spring samples is given in Figure 5. An almost linear tendency with positive slope is observed which supports the occurrence of a mixing process in the system. Mixing models were reviewed by Fournier (1979b, 1992). Silica and chloride concentration of springs, enthalpy of springs and reservoir temperature calculated by geothermometers are used to obtain the chloride and silica concentration for the hot member. Sample TU35 was selected as the cold member and a reservoir temperature of 230°C was taken to carry out modelling.

Figure 6 is a silica vs. specific enthalpy plot, where the samples have been represented as well as the quartz solubility curve. A linear tendency for the samples is observed which shows the occurrence of a mixing process. The fitted straight line for the samples were calculated by the minimum square method. This line is explained by assuming that reservoir liquid at 230°C is cooled to 166°C by boiling and subsequently it mixes with non-thermal waters to give the spring compositions. This boiling process is shown by moving the point

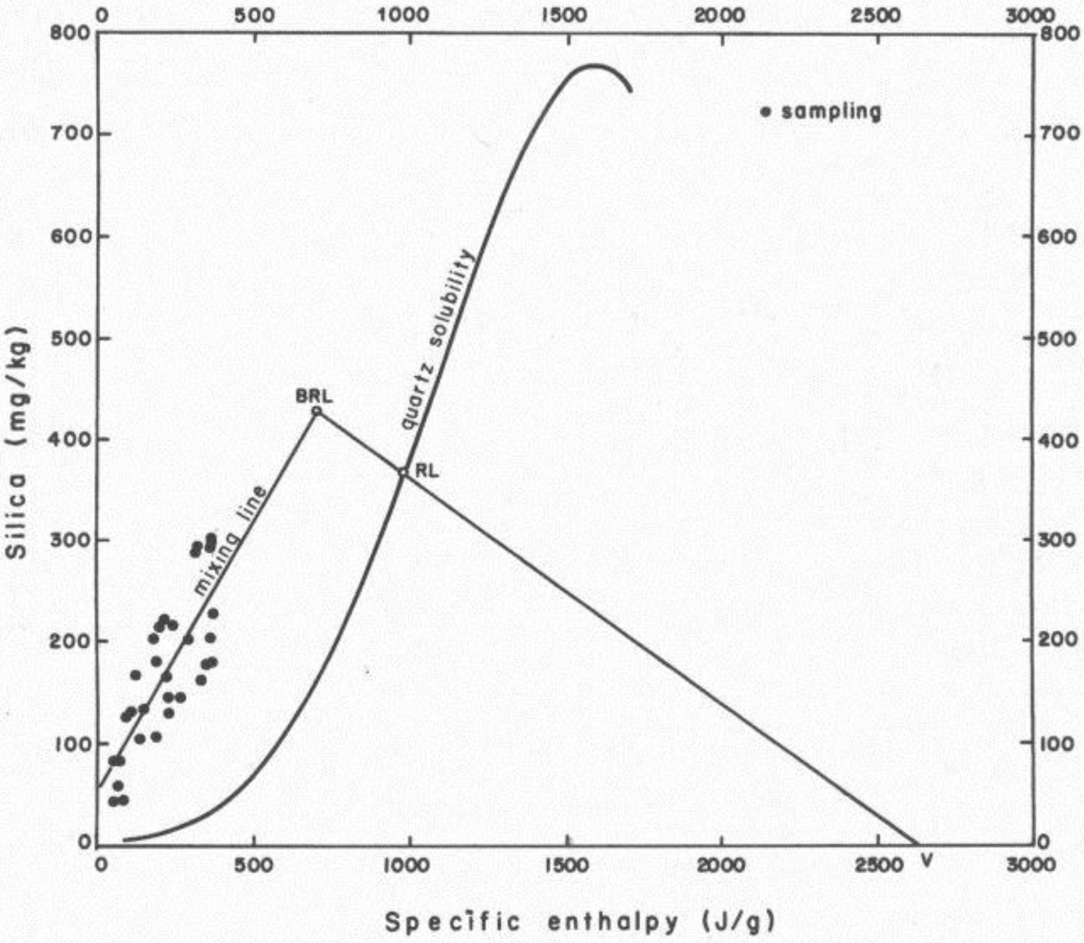

Figure 6. Silica vs. specific enthalpy diagram

RL (reservoir liquid) to the point BRL (boiled reservoir liquid). The point for separated vapour is *V*. From this diagram the silica concentration for the reservoir liquid is estimated as 376·4 mg/kg and the specific enthalpy as 990·1 J/g. For the boiled reservoir liquid a silica concentration of 430·2 mg/kg and a specific enthalpy of 701·7 J/g were estimated.

Figure 7 is a specific enthalpy vs. chloride plot. Points for the samples were fitted by the minimum square method and the straight line which shows the mixing process was also represented. Sample RC15 was taken as the end member for fitting considering that it was sampled at boiling temperature such as samples AN2, AN3, AN4, KA, RC1 and RC12. Sample RC15 has the lowest chloride concentration at boiling temperature. Cooling processes that explain higher chloride contents than sample RC15 must be different than single mixing as it will be discussed later. For a reservoir temperature of 230°C (point RL), boiling is represented by a straight line starting on the point *V* which represents the separated vapour. This boiling line intercepts the mixing line on the point BRL (boiled reservoir liquid) which occurs at a temperature of 166°C. This previously found temperature is the intercept of boiling and mixing lines for the silica-enthalpy model. For the reservoir liquid the chloride concentration was found to be 2576 mg/kg, while for the boiled liquid it was estimated as 2983 mg/kg. A second boiling process after mixing could explain the high chloride samples AN2,

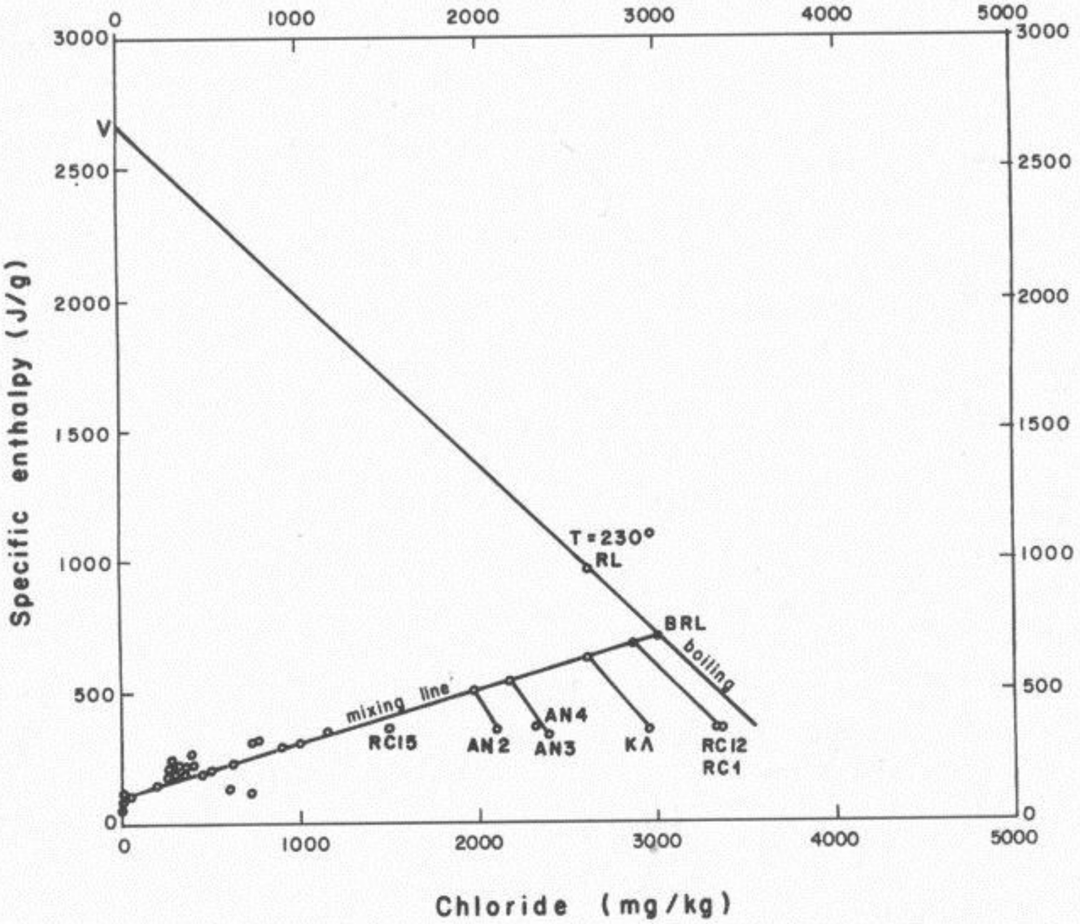

Figure 7. Specific enthalpy vs. chloride diagram

AN3, AN4, KA, RC1 and RC12. In the diagram such boiling processes are represented by straight lines starting on the point referred to separated vapour (*V*). The lines cross the mixing line providing the chloride and enthalpy for the mixed parent liquid. The highest chloride concentration of a spring coming from the reservoir without mixing would be 3500 mg/kg.

The fraction of hot component for spring samples was calculated considering mass and enthalpy balances. Figure 8 gives the results obtained by silica vs. enthalpy balances and Figure 9 shows the results for chloride vs. enthalpy balances. The results seem to compare well. For sample RC15 a hot member fraction of about 0·45 was obtained, for higher chloride samples that fraction is still higher.

6. ISOTOPIC RESULTS

Isotopic results ($\delta^{18}O$ and δD) of some spring samples from Tutupaca and Río Calientes-Ancocollo-Challapalca zones are shown in Figure 10. One sample from other interesting zone named Vilacota was included (PV-2). The isotopic analyses were performed by the International Atomic Energy Agency (IAEA) and the IIE as indicated. As seen in Figure 10, an oxygen-18 shift of about two units is shown for the samples from Río Calientes-Ancocollo regarding the samples from Tutupaca and Vilacota

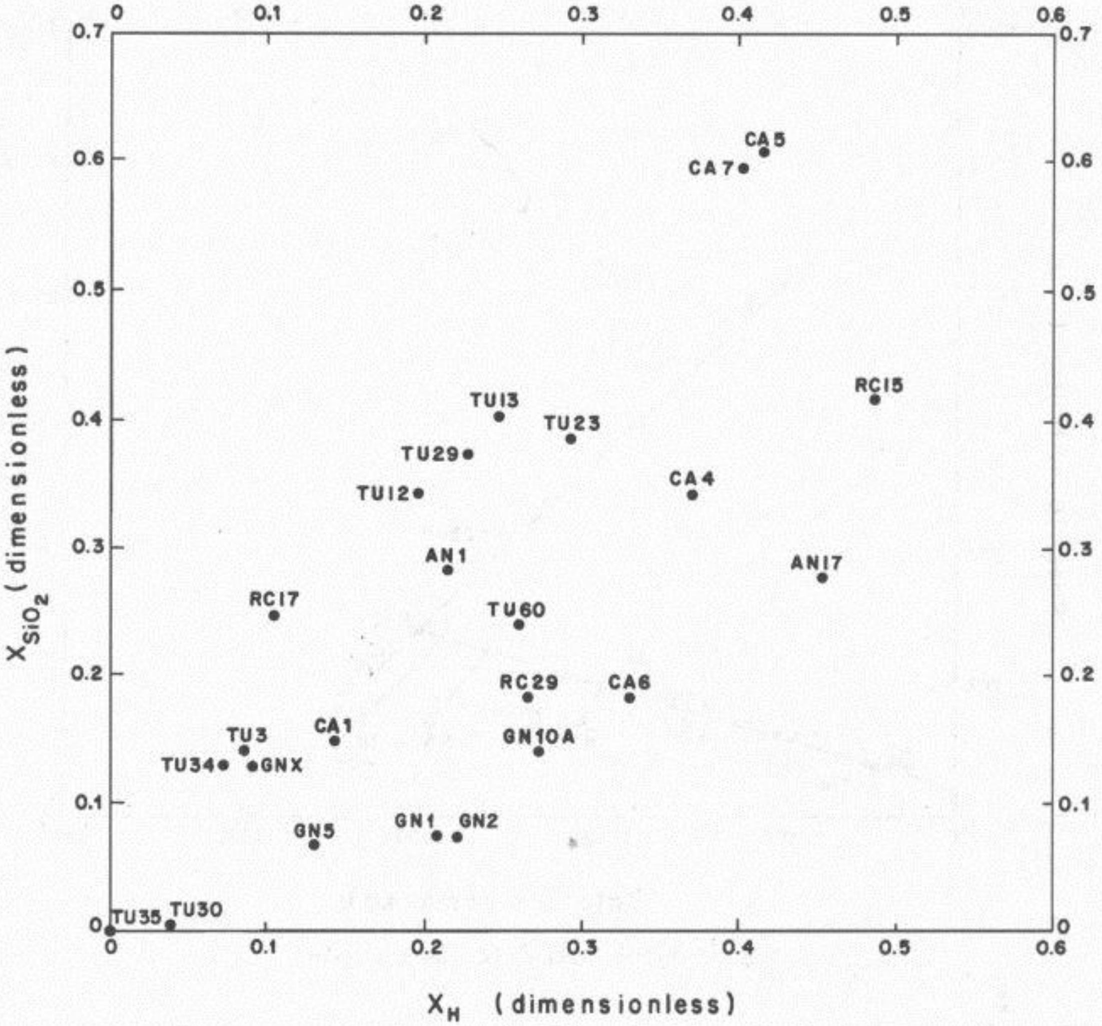

Figure 8. Fraction of hot component based on silica balance vs. fraction of hot component based on enthalpy balance for the springs

which are located in the world meteoric line trend. This shift characteristic of high temperature geothermal waters.

7. CONCLUSIONS

Analysis of spring chemical data from Republic of Peru suggests that one or more geothermal reservoirs could occur. Typical acidic sulphate springs located in Tutupaca region are probably heated by magmatic gases. Almost neutral chloride springs located in Río Calientes-Ancocollo-Challapalca zone were classified as 'mature' waters. Chemical geothermometers provided a wide range of temperatures for the reservoir, which was due to the lack of full water–rock equilibrium in the system. A reservoir temperature in the range 210–240°C was estimated by using an approach that considers Na–K–Ca–Mg content for the springs.

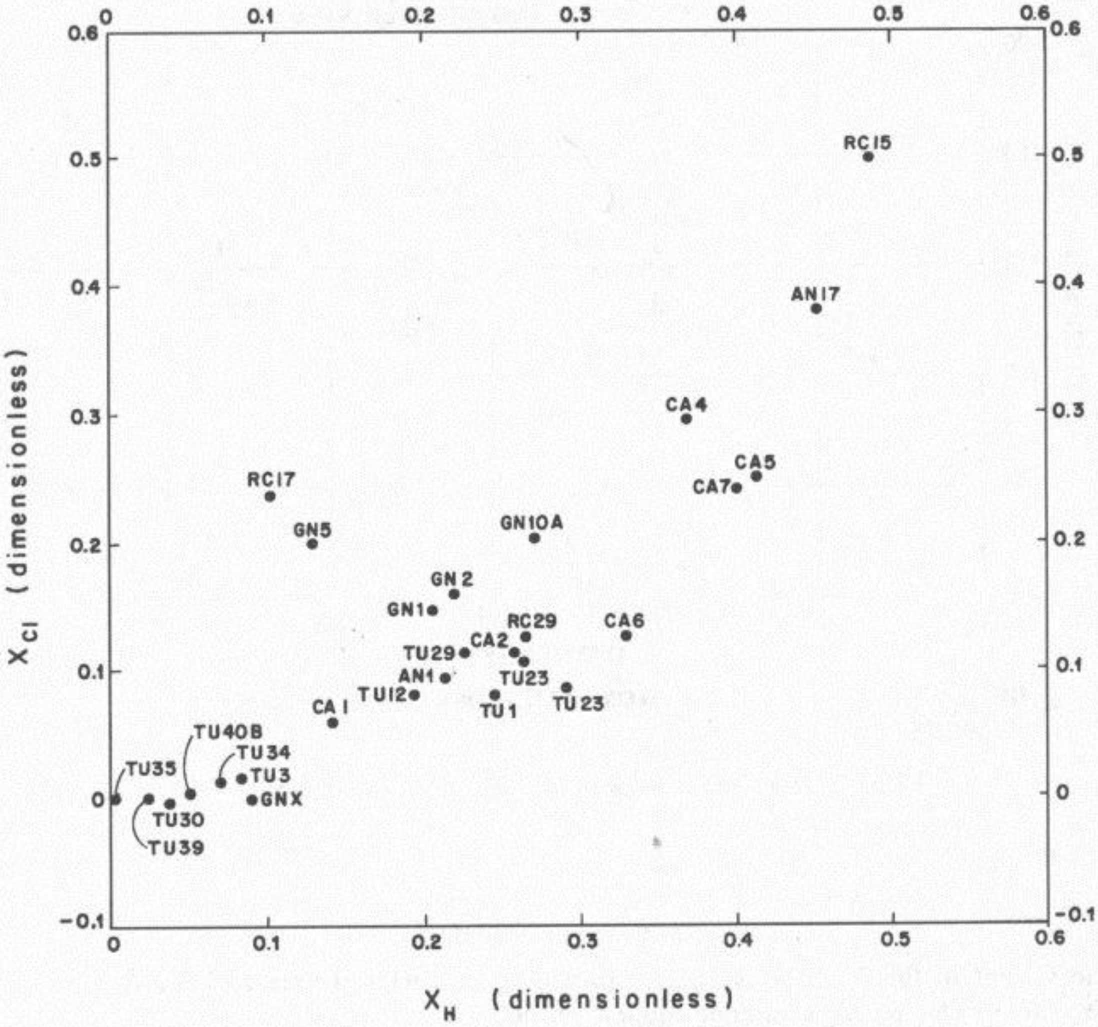

Figure 9. Fraction of hot component based on chloride balance vs. fraction of hot component based on enthalpy balance for the springs

Mixing modelling based on silica-enthalpy and enthalpy-chloride diagrams was carried out for a reservoir temperature of 230°C. For both models it can be stated that the reservoir fluid is firstly cooled by boiling at 166°C. Boiled liquid is then mixed with non-thermal waters to give the observed spring compositions. It is proposed that some high chloride samples from Río Calientes-Ancocollo-Challapalca are cooled by an additional boiling process after mixing. This fact was observed to occur especially in the Río Calientes zone where intermitent steam separation in the pools was observed when sampling.

Isotopic results (oxygen and deuterium) show that samples from Tutupaca and Vilacota are located in the world meteoric line while samples from Río Calientes-Ancocollo-Challapalca show an oxygen shift of about two units. This is characteristic of geothermal waters from high-temperature reservoirs.

It is concluded that commercial exploitation of the Río Calientes zone is feasible by means of conventional or binary system. In order to obtain accurate physicochemical characteristics of deep fluids, drilling is recommended. This also provides a better knowledge of geologic conditions of the zone.

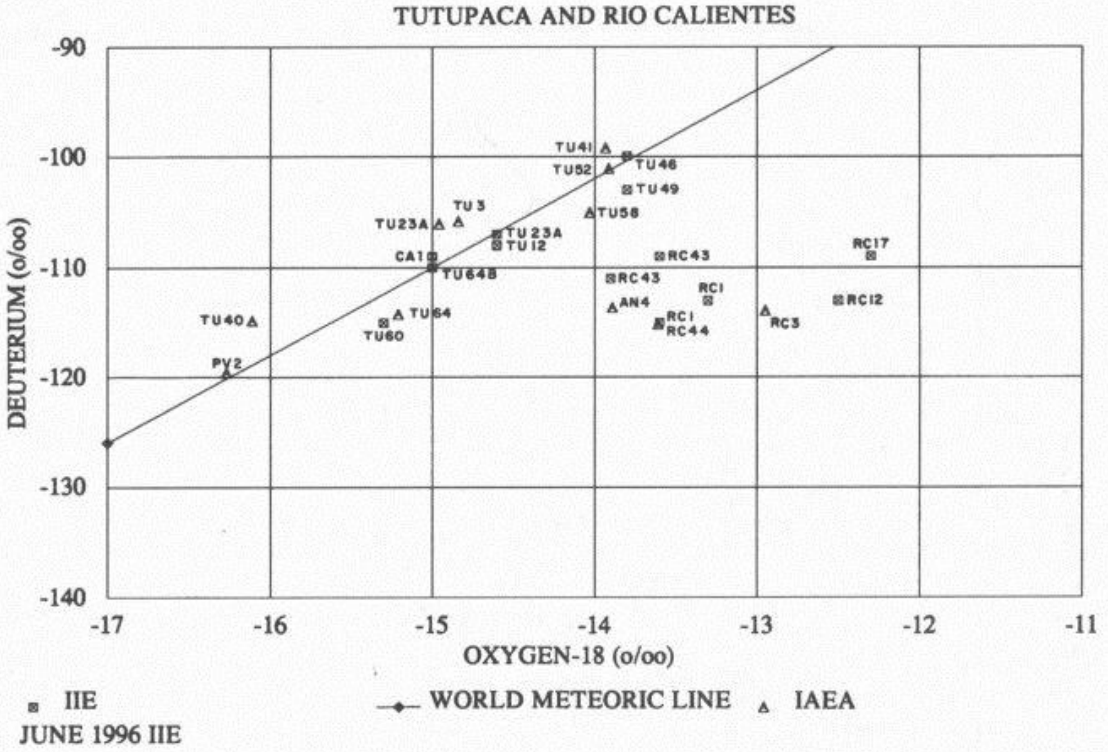

Figure 10. Deuterium vs. oxygen-18 (in permil SMOW) of the spring waters

ACKNOWLEDGEMENTS

The authors want to thank CENERGIA for providing geochemical data and Secretaría de Relaciones Exteriores (México) for partial economic support of the study.

REFERENCES

Barragán, R. R. M., Arellano, G. V. M., Birkle, P., González, P. E., Santoyo, E. and Torres, R. V. (1996). 'Análisis de información geoquímica de zonas geotérmicas en el SE de la República de Perú', *Internal Report, Instituto de Investigaciones Eléctricas, prepared for ELECTROPERÚ*, 87 p.

Birkle, P., González, P. E., Torres, R. V. and Barragán, R. M. (1996). 'Estudio geológico y estructural sobre el potencial geotérmico del área del lote Tutupaca en el sur de Perú', *Internal Report, Instituto de investigaciones Eléctricas prepared for ELECTROPERÚ*, 25 p.

ELECTROPERÚ S. A. (1994). 'Estudio geovolcalógico e inventario sistemático de manifestaciones geotermales del lote Tutupaca. Hidrogeología, hidrogeoquímica y áreas de interés', *Internal Report*, Perú, pp. 264–300.

Fournier, R. O. and Truesdell, A. H. (1973). 'An empirical Na–K– Ca geothermometer for natural waters', *Geochim. Cosmochim. Acta*, **37**, 1255–1275.

Fournier, R. O. (1979a). 'A revised equation for the Na/K geothermometer', *Geotech. Res. Council Trans.*, **3**, 221–224.

Fournier, R. O. and Potter II, R. W. (1979). 'Magnesium correction to the Na–K– Ca chemical geothermometer', *Geochim. Cosmochim. Acta*, **43**, 1543–1550.

Fournier, R. O. (1979b). 'Geochemical and hydrological considerations and the use of enthalpy-chloride diagrams in the prediction of underground conditions in hot-spring system', *J. Volcanol. Geotherm. Res.*, **5**, 1–16.

Fournier, R. O. and Potter II, R. W. (1982). 'A revised and expanded silica (quartz) geothermometer', *Geoth. Res. Council Bull.*, **11–10**, 3–12.

Fournier, R. O. (1992). 'Water geothermometers applied to geothermal energy', In *Application of Geochemistry in Geothermal Resevoir Development*, F. D'Amore (Ed.), UNITAR/UNDP, Rome, pp. 37– 69.

Giggenbach, W. F. (1991). 'Chemical techniques in geothermal exploration', In *Application of Geochemistry in Geothermal Resevoir Development*, F. D'Amore (Ed.), UNITAR/UNDP, Rome, pp. 119–142.

Giggenbach, W. F. (1988). 'Geothermal solute equilibria. Derivation of Na–K–Mg geoindicators', *Geochim. Cosmochim. Acta*, **52**, 2749–2765.

Giggenbach, W. F. (1995). 'Geochemical exploration of a "difficult" geothermal system, Paraso, Vella Lavella, Solomon Islands', *Proc. World Geothermal Congress*, Vol. 2, Italy, pp. 995–1000.

Mercado, S. and Nieva, D. (1980). 'Interpretación geoquímica de zonas de alteración hidrotermal de la República de Perú', *Internal Report*, Instituto de Investigaciones Eléctricas, Cuernavaca, México, IIE/FE-G23/2.

Nieva, D. and Nieva, R. (1987). 'Developments of geothermal energy in México, Part twelve— a cationic composition geothermometer for prospecting of geothermal resources', *Heat Recovery Systems CHP*, **7**, 243–258.